Electronic Supplementary Material (ESI) for Chemical Science.
This journal is © The Royal Society of Chemistry 2024

Electronic Supplementary Information

Integrated "Rigid-Flexible" Strategy by Side Chain Engineering towards High Ion-Conduction Cationic Covalent Organic Framework Electrolytes

Jian Song, Li Lin, Fengchao Cui, Heng-Guo Wang, Yuyang Tian,* and Guangshan Zhu*

Experimental Section

Materials

All starting materials and organic solvents were purchased from commercial suppliers and used without further purification unless otherwise noted. All reactions were performed in oven-dried glassware under nitrogen or argon atmosphere using standard Schlenk and glovebox techniques.

General instrumentation and methods

^{1}H NMR spectra were recorded on Varian Inova 500 MHz NMR spectrometer. ^{13}C CP/MAS solid-state NMR spectra were obtained using a Bruker Avance III model 400 MHz NMR spectrometer at a MAS rate of 5 kHz. FT-IR measurements were performed on the Nicolet IS50 Fourier transforms infrared spectrometer. The Elemental analyses (for C, H, and N) were measured using a Perkin Elmer 2400 Series II CHNS/O Analyzer. TGA were measured on the METTLER-TOLEDO TGA/DSC 3+ analyzer at the 10 ℃ min^{-1} heating rate in air atmosphere. N_2-adsorption isotherms and pore size distribution were obtained at 77 K using an Autosorb iQ2 adsorptometer, Quantachrome Instrument. The scanning electron microscopy (SEM) images were acquired by the field emission scanning electron microscopy (FE-SEM, SU-8010, Hitachi). Transmission electron microscopic (TEM) images were generated with JEOL JEM-2100 instrument at an accelerating voltage of 200 kV. The powder X-ray diffraction (PXRD) measurements were carried out on the Dmax2200PC X-ray diffractometer with Cu-Kα radiation (40 kV, 30 mA, λ = 1.5418 Å) and a scanning step of 0.01°. X-ray photoelectron spectroscopy (XPS) were recorded on an Escalab-MK II photoelectronic Spectrometer with Al Kα (1200 eV).

Synthetic Procedure

Synthesis of BIm-COF. A Pyrex tube was charged with 4,4′,4″,4‴-(ethene-1,1,2,2-tetrayl)tetraaniline (ETTA)

(7.8 mg, 0.02 mmol), 4,4′-(1-methyl-1H-benzo[d]imidazole-4,7-diyl)dibenzaldehyde (BImDB) (13.6 mg, 0.04 mmol), o-dichlorobenzene (0.75 mL), n-butanol (0.25 mL), and 6 M aqueous acetic acid (0.1 mL). The tube was degassed by freeze-pump-thaw technique for three times and then sealed under vacuum. The reaction was heated at 120 ℃ for 3 days yielding solid at the bottom of the tube. The resulting yellow precipitate was filtered off and washed with dichloromethane, tetrahydrofuran, and methanol, respectively, then Soxhlet extracted with THF for 48 h. The product was dried at 80 ℃ under vacuum for overnight to obtain BIm-COF (Yield: 80%).

Synthesis of 3-(2-(2-(2-methoxyethoxy)ethoxy)ethyl)-1-methyl-1*H*-benzo[*d*]imidazolium Bromide (EO-BIm). 1-methylbenzimidazole (100 mg, 0.757 mmol), diethylene glycol 2-bromoethyl methyl ether (1.87 mL, 7.57 mmol), and anhydrous acetonitrile (10 mL) were added into Teflonlined autoclaves at 120 ℃ for 24 h. Then vacuum rotatory evaporator was used for the concentration, and extracted with hexane to obtain brown oil product (>99% yields). ^{1}H NMR (CD_3OD, 500 MHz): δ (ppm) 9.41 (1H), 7.93 (1H), 7.87 (1H), 7.63 (2H), 4.73 (2H), 4.62 (2H), 4.08 (3H), 3.86 (2H), 3.50 (2H), 3.45 (2H), 3.40 (2H),3.22 (3H).

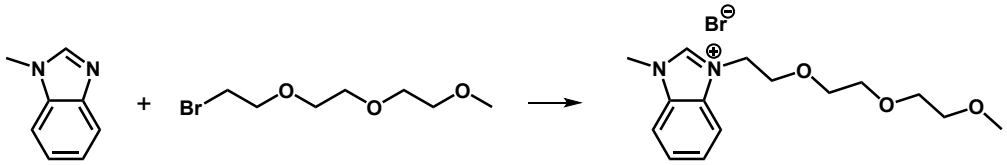

Fig. S1 Schematic route to the synthesis of the EO-modified model compound.

Synthesis of EO-BIm-iCOF. BIm-COF (500 mg), diethylene glycol 2-bromoethyl methyl ether (2.48 mL), and anhydrous acetonitrile (10 mL) were added into Teflonlined autoclaves at 120 ℃ for 24 h. After filtration, the product was washed with anhydrous acetonitrile and methanol, respectively, to afford a brown powder **EO-BIm-iCOF(Br)** (712 mg, 98% yields). The **EO-BIm-iCOF(Br)** powder was dispersed and stirred in a 15wt% LiTFSI aqueous solution (50 mL) at 50 ℃ for ion exchange. The solution was changed with the fresh LiTFSI solution every 24 hours for three times. The olive-green solid product was filtered and washed with deionized water and ethanol for several times (named as **EO-BIm-iCOF**).

Synthesis of LiTFSI@EO-BIm-iCOF. After ion exchange, the product EO-BIm-iCOF (600 mg) was mixed with LiTFSI (93 mg) in 15 mL ethanol solvent. After stirring for 12 hours, the solvent is removed by a rotary evaporator. The final product was dried at 80 ℃ in vacuum overnight and stored in the glovebox.

Electrochemical performance

The COFs solid-state electrolytes were prepared by loading with LiTFSI salts through the solution diffusion method based on the molar ratio of 1:1 between N^+ (corresponding to the cationic methylimidazole in the framework) and Li^+ to yield LiTFSI@EO-BIm-iCOF and LiTFSI@BIm-COF, respectively. ~20 mg of the LiTFSI@COFs sample was loaded into a die (Φ14 mm) and pressed into a solid-state electrolyte pellet.

Ionic conductivities measurement. The stainless-steel (SS) symmetric SS‖LiTFSI@EO-BIm-iCOF‖SS CR2032 coin-type cell was assembled and used to measure the ionic conductivity by electrochemical impedance spectroscopy (EIS). EIS was conducted using an electrochemical workstation (Autolab PGSTAT302N) in the temperature range of 303-358 K with a frequency of 1 Hz to 10^6 Hz. The ionic conductivity was calculated using $\sigma = L/(R \times S)$, where R (Ω) is the is the bulk resistance in the Nyquist plot, L (cm) is the thickness of LiTFSI@EO-BIm-iCOF pellet, and S (cm^2) is the surface area. The activation energy was calculated from the conductivities as a function of temperature using the Arrhenius equation:

$$\sigma T = \sigma_0 \exp\left(\frac{-E_a}{k_B T}\right)$$

Where σ and σ_0 denote ionic conductivity and pre-exponential factor, respectively, T indicates the absolute temperature in kelvin, Ea indicates the activation energy and k_B denotes the Boltzmann constant.

Lithium-ion transference number. LiTFSI@EO-BIm-iCOF solid-state electrolyte was sandwiched between two lithium foils. The resulting Li‖LiTFSI@EO-BIm-iCOF‖Li CR2032 coin-type cells were set up to be analyzed. First, an AC impedance test was performed to obtain the initial resistance (R_0) with the range of the frequency from 0.01 Hz to 10^6 Hz. The symmetric cell was then subjected to a constant DC voltage (ΔV, 10 mV), during which the initial current (I_0) was monitored until reaching the steady state current (I_{ss}). Another AC impedance test was then conducted to obtain the steady state resistance (R_{ss}) with the range of the frequency from 0.01 Hz to 10^6 Hz.

Li-ion transference number (t_{Li^+}) was calculated according to the following equation:

$$t_{Li^+} = \frac{I_{ss}}{I_0} \times \frac{\Delta V - I_0 R_0}{\Delta V - I_{ss} R_{ss}}$$

ΔV: Polarization voltage (in the case of this work, ΔV = 10 mV).

I_0: The initial current.

I_{ss}: The steady state current.

R_0: The resistance before the polarization.

R_{ss}: The resistance after the steady state.

Linear sweep voltammetry (LSV). Linear sweep voltammetry (LSV) was carried out to determine the electrochemical stability window by electrochemical workstation (Autolab PGSTAT302N). LiTFSI@EO-BIm-iCOF solid-state electrolyte was sandwiched by a Li foil electrode and a stainless-steel (SS) electrode to assemble a SS‖LiTFSI@EO-BIm-iCOF‖Li CR2032 coin-type cell. The sweep speed was set as 1 mV s^{-1} in the range of 2 to 5 V.

Performance of $LiFePO_4$‖LiTFSI@EO-BIm-iCOF‖Li cell

The integrated solid-state lithium battery was prepared using LiTFSI@EO-BIm-iCOF as electrolyte, $LiFePO_4$ as cathode material, and Li metal as anode and in CR2032 coin-type cells. The cathodes were prepared by homogenously blending $LiFePO_4$, acetylene black, and poly(vinylidene fluoride) (PVDF) with a mass ratio of 8:1:1 in NMP. The resulting slurry was uniformly coated on an aluminum foil and dried in a vacuum oven at 70 ℃ for 12 h. All the above operations were carried out in the glovebox. To reduce interfacial resistance in the solid-state LIBs, a trace amount of LiTFSI electrolyte (10 μL, 1M LiTFSI in a mixture of ethylene carbonate (EC), dimethyl carbonate (DMC) and ethyl methyl carbonate (EMC) in the volume ratio of 1:1:1) was dropped on the surface of the solid-state electrolyte pellet. Charge and discharge curves, cycling stability at different rate, and rate capability of SSLIB were performed at 2.5-4.3 V (LANHE CT3001A battery testing system at 30 ℃).

Theoretical calculation method

The molecular dynamics were performed using the software package GROMACS (version 2021.3).[1-4] The molecules (LiTFSI, $TFSI^-$) were optimized in Gaussian 16 first. The system is composed of COF and a certain amount of lithium salts (LiTFSI), and the amount of lithium salts is consistent with the molar amount of imidazole groups in the main COF skeleton. The atomic interactions of molecules were parameterized by the optimized potentials for liquid simulations all-atom (OPLS-AA) force field,[5] and RESP2 charge obtained from Multiwfn[6] was applied in the calculations. The atomic interactions of COF framework were parameterized by universe force field (UFF). After the energy minimization, the systems were pre-balanced in NVT ensemble with v-rescale thermostat for 10 ns. Then, the production run was carried out in the NVT ensemble at 300 K with the time step of 1 fs. The temperature of the system was controlled by a nose-hoover thermostat (τT=1 ps). After 50 ns of simulation, the MSD and RDF of the particles were analyzed by the toolkits of GROMACS.

Results and Discussion

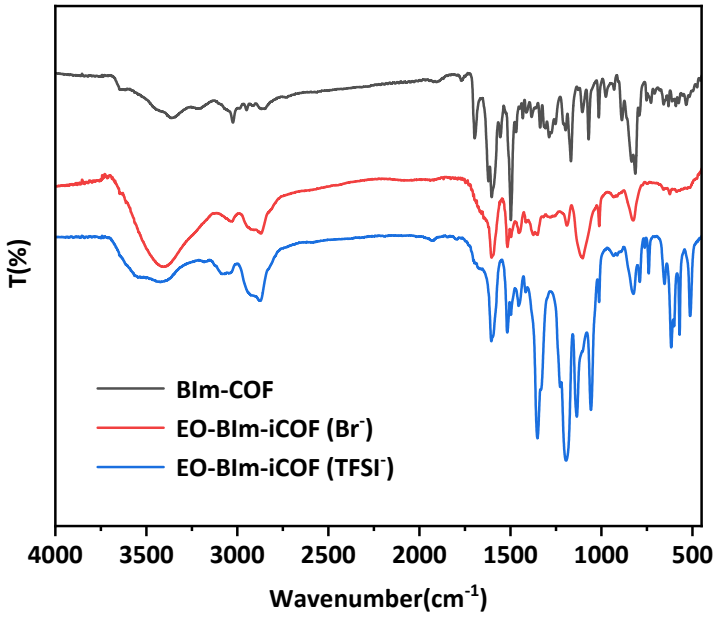

Fig. S2 FT-IR spectra of BIm-COF, EO-BIm-iCOF(Br^-) and EO-BIm-iCOF($TFSI^-$).

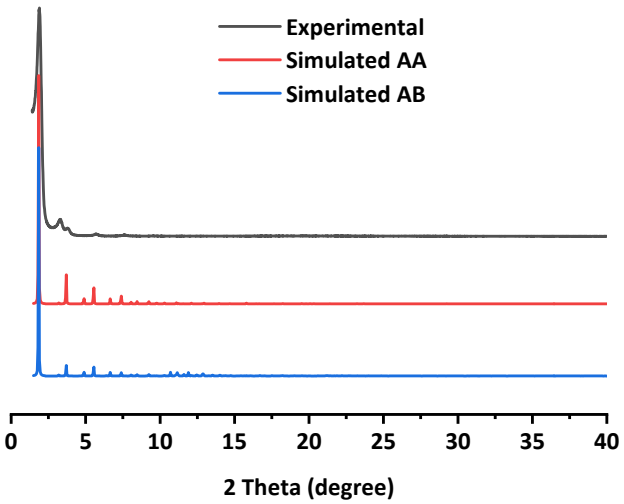

Fig. S3 PXRD patterns of as-synthesized BIm-COF, the experimental (black), the corresponding simulated AA stacking structure (red), and simulated AB stacking structure (blue).

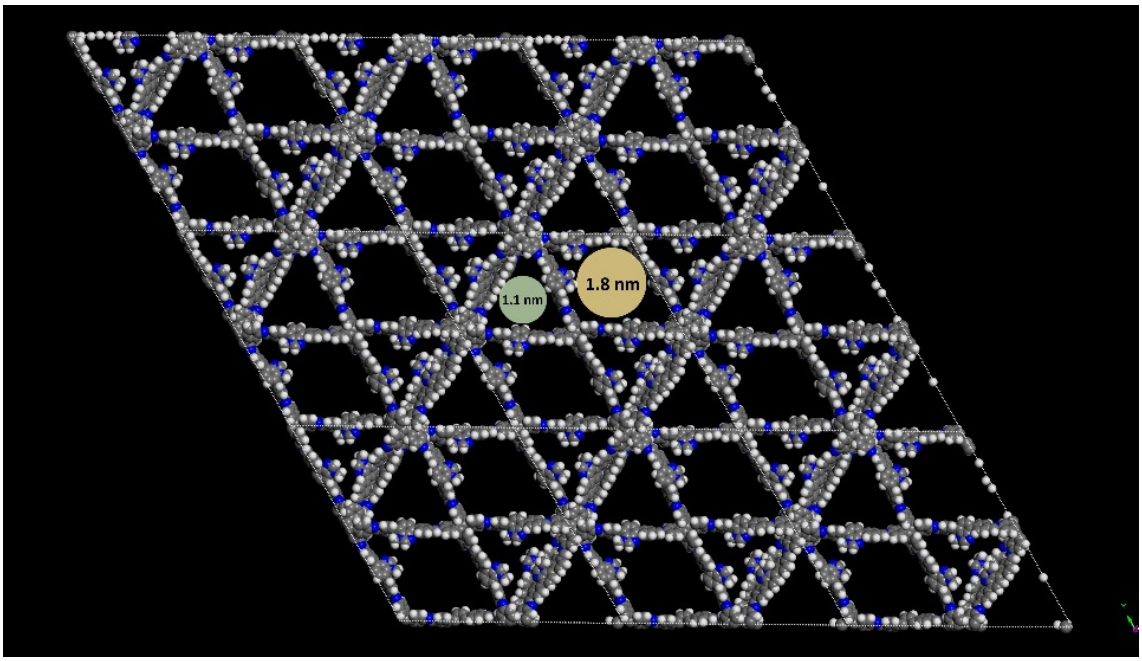

Fig. S4 The AB-stacking model of BIm-COF.

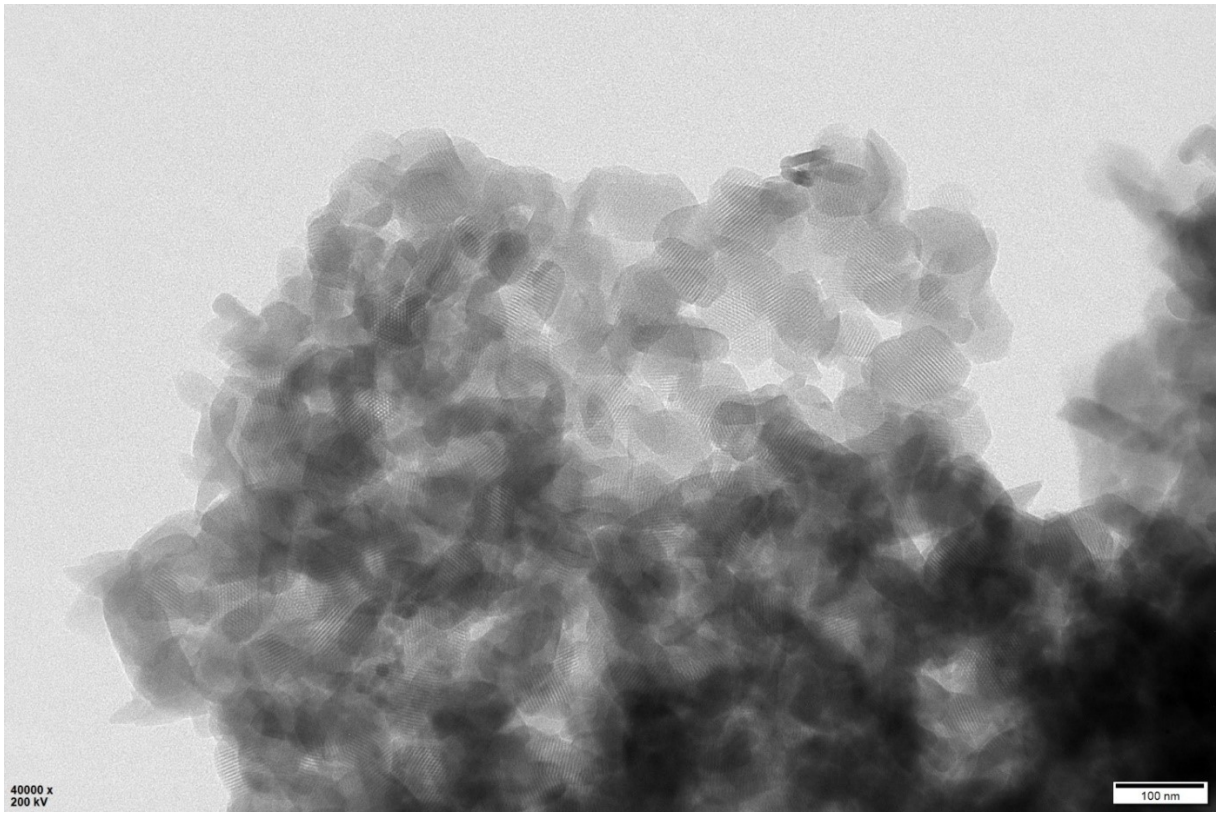

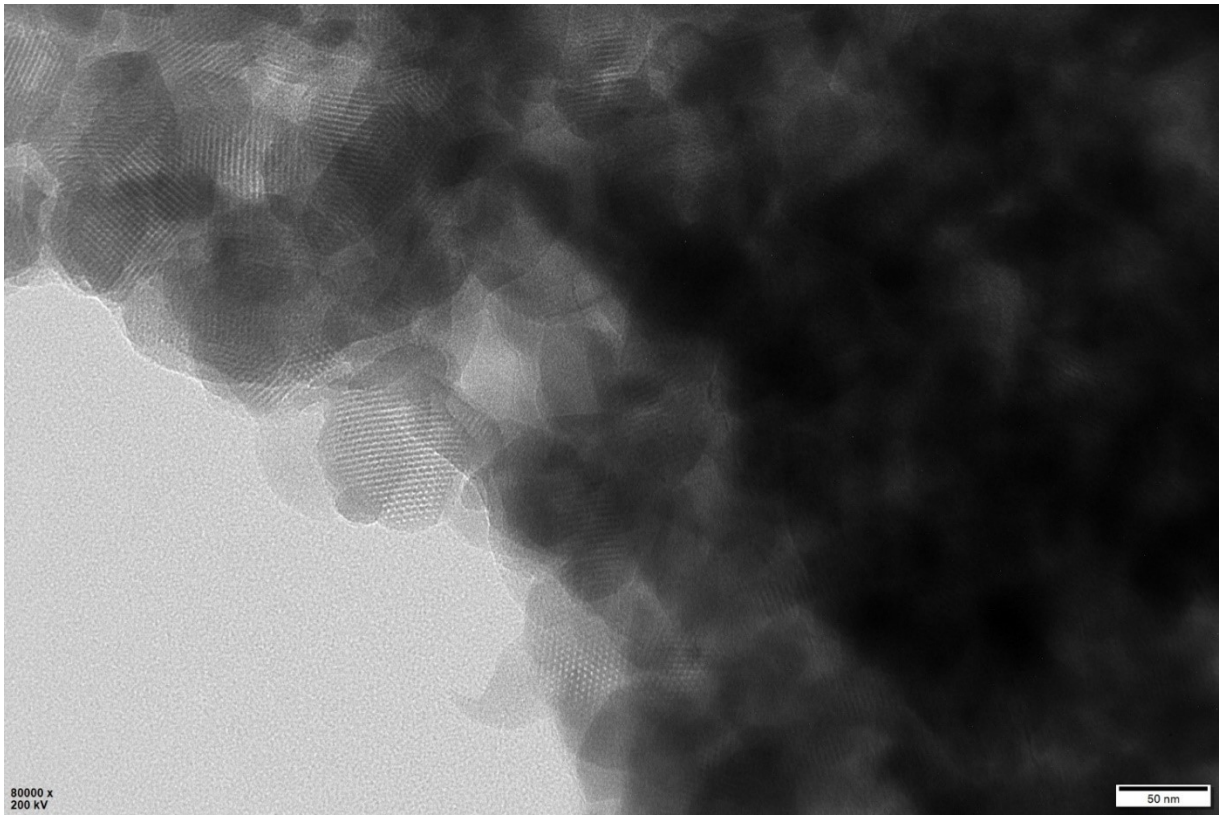

Fig. S5 TEM images of BIm-COF.

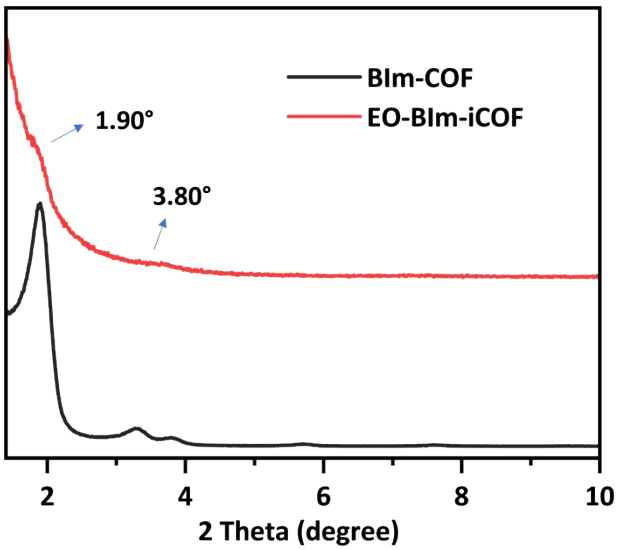

Fig. S6 Experimental PXRD patterns of BIm-COF and EO-BIm-iCOF.

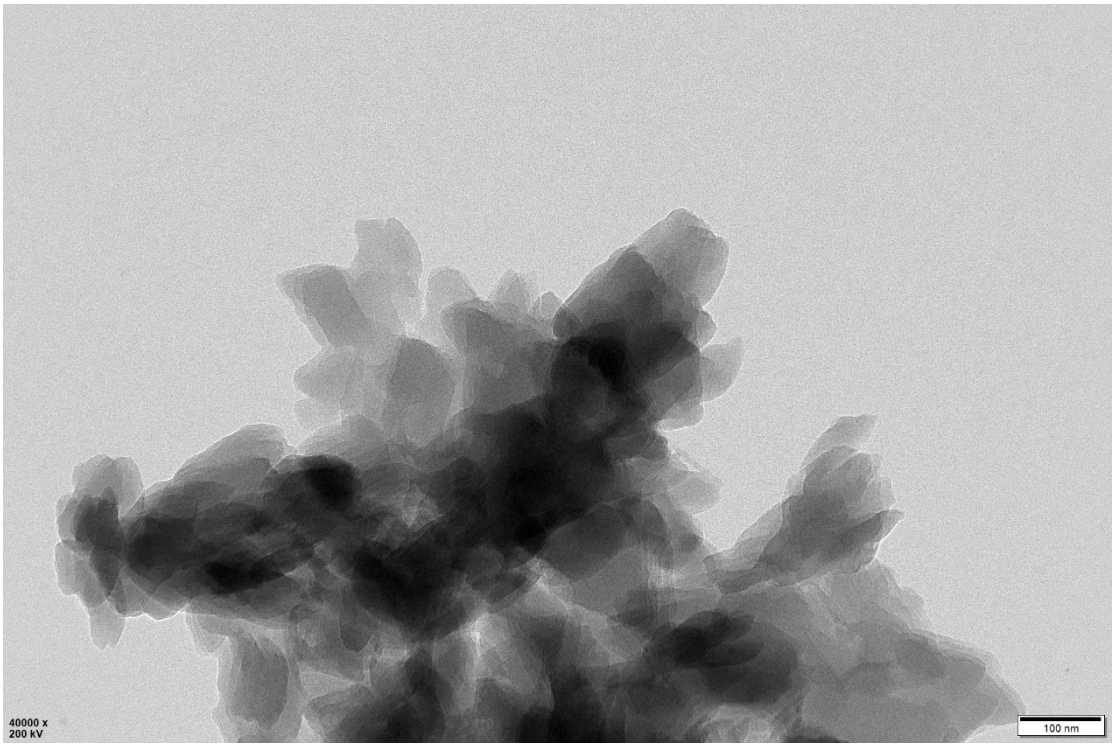

Fig. S7 TEM image of EO-BIm-iCOF.

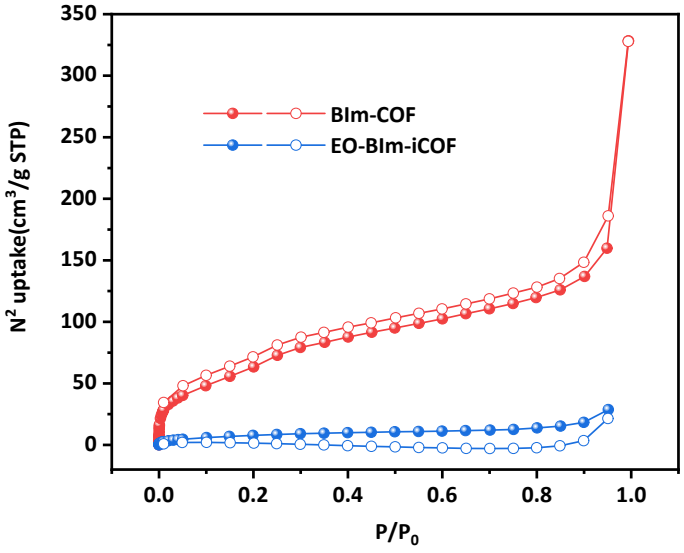

Fig. S8 N_2 adsorption (filled symbol) and desorption (open symbol) isotherm curves of as-synthesized BIm-COF and EO-BIm-iCOF measured at 77 K.

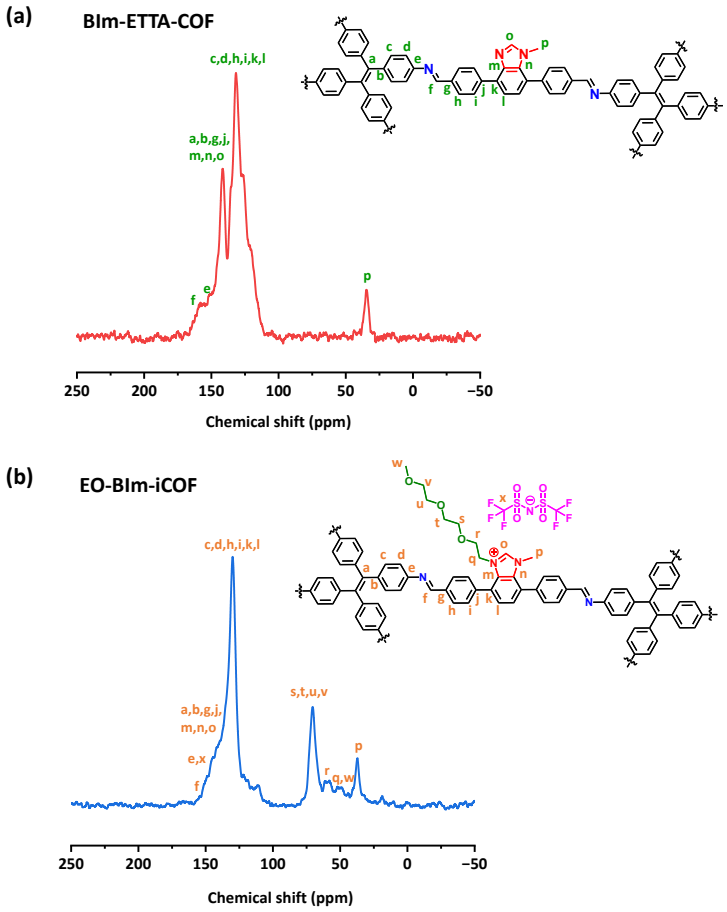

Fig. S9 ^{13}C CP/MAS solid-state NMR spectra of BIm-COF and EO-BIm-iCOF.

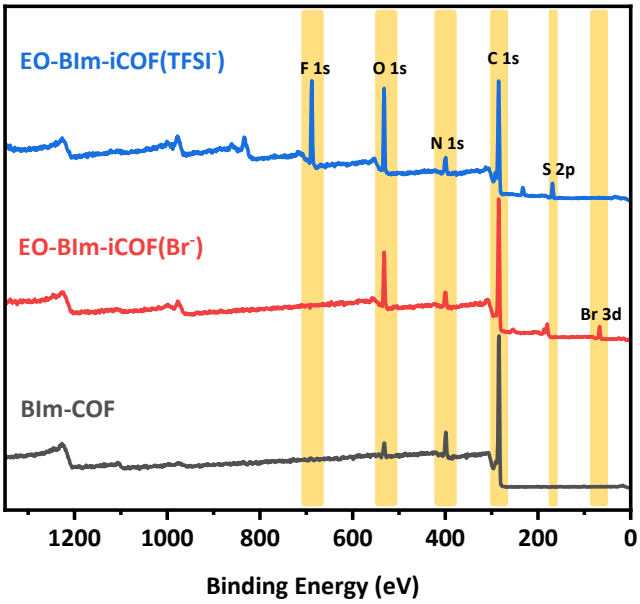

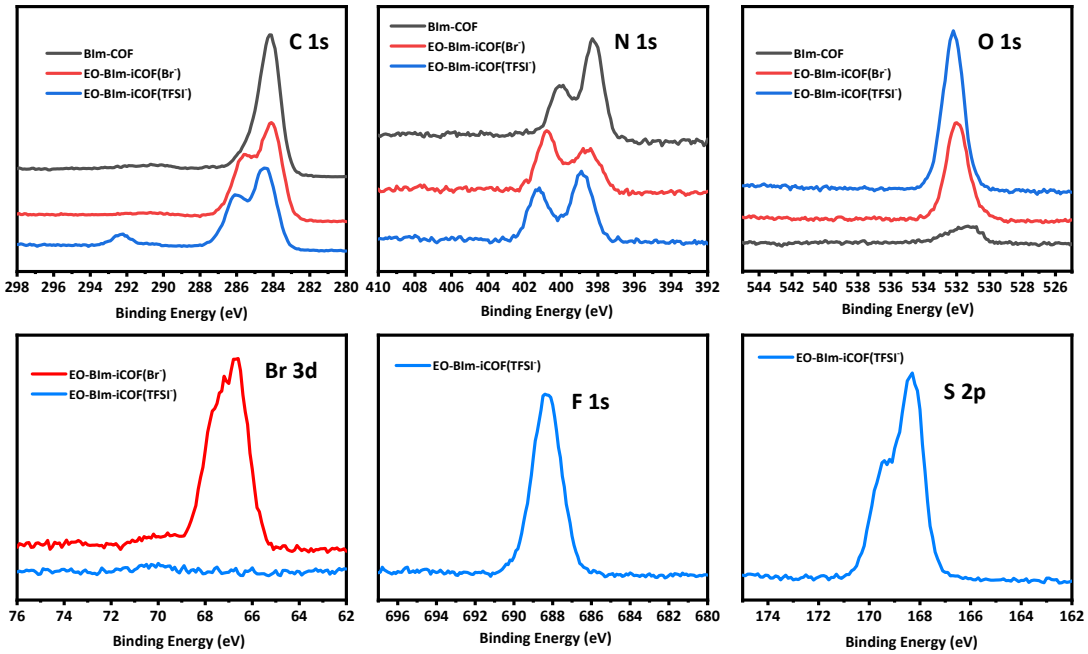

Fig. S10 XPS spectra of BIm-COF and EO-BIm-iCOF.

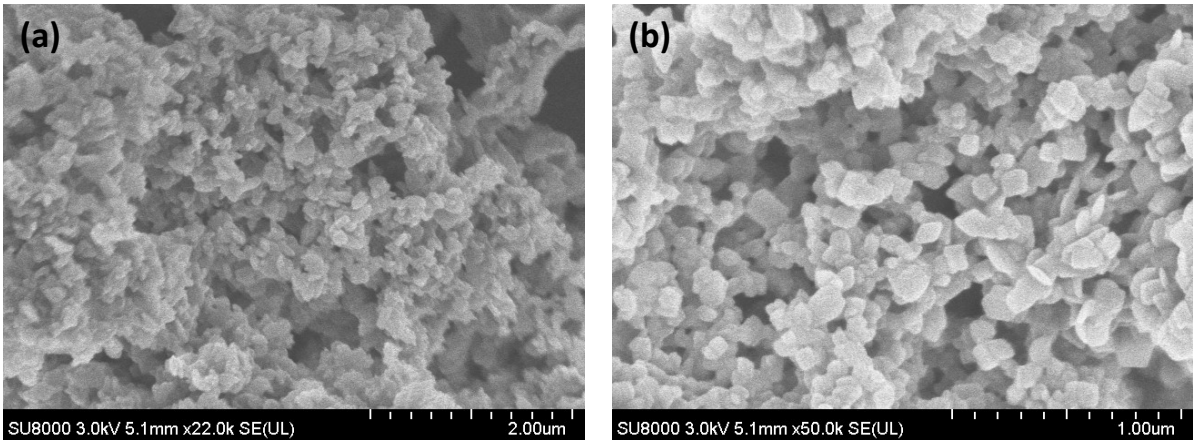

Fig. S11 SEM images of BIm-COF (a) and EO-BIm-iCOF (b).

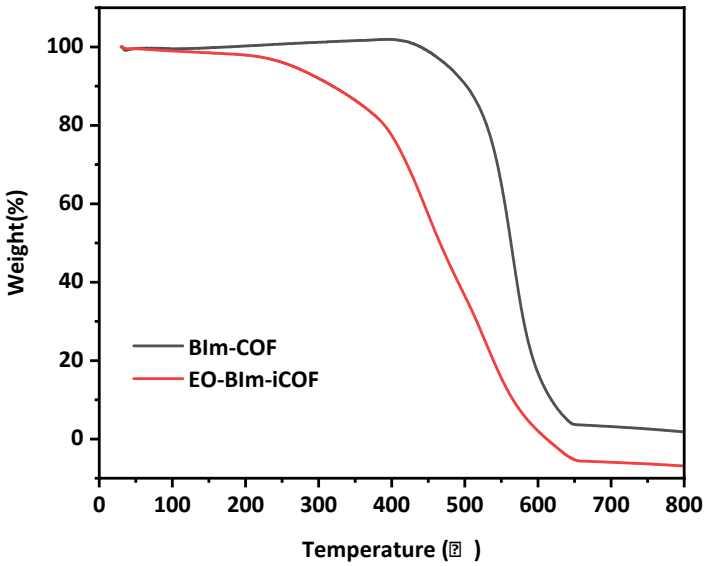

Fig. S12 TG curves of BIm-COF and EO-BIm-iCOF.

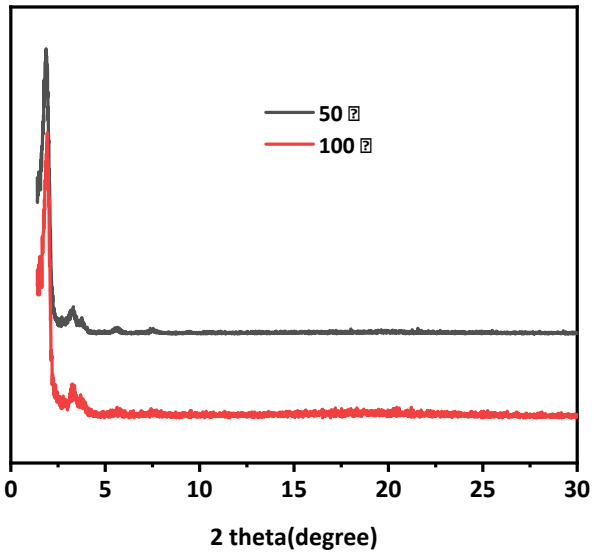

Fig. S13 Experimental PXRD patterns of BIm-COF after 50 ℃ and 100 ℃ heat treatment.

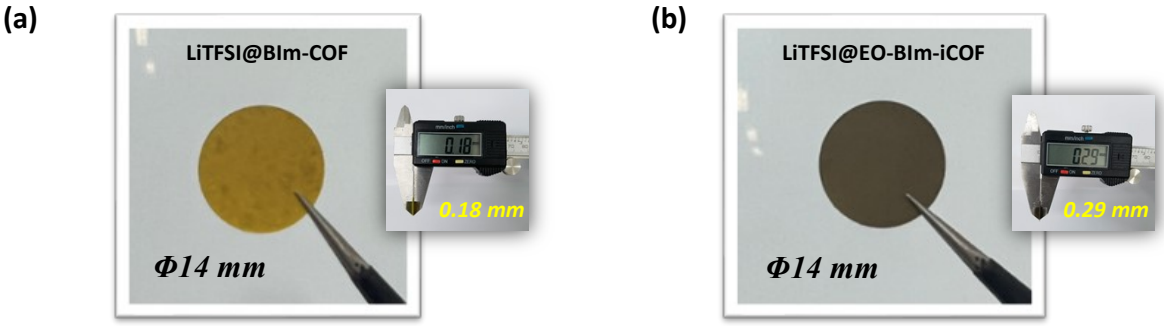

Fig. S14 Digital photos of LiTFSI@COFs solid-state electrolyte pellets.

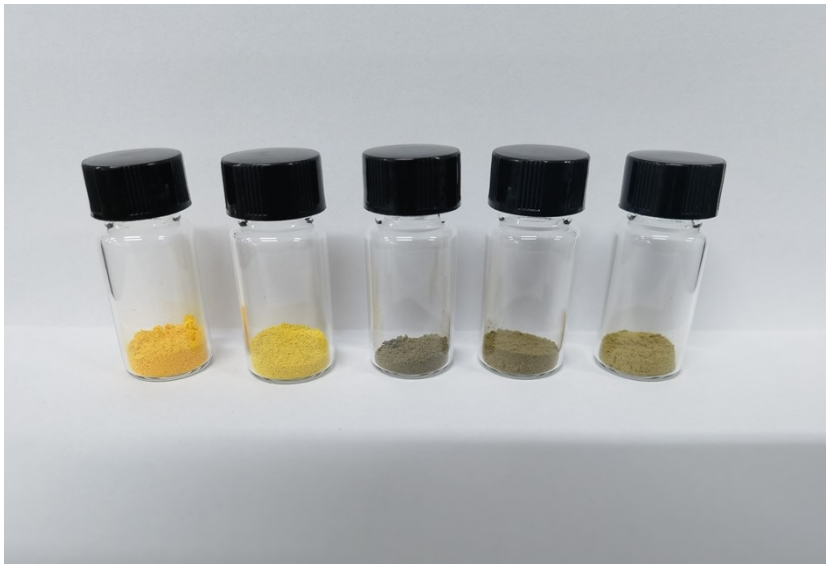

Fig. S15 The sample photos of BIm-COF, LITFSI@BIm-COF, EO-BIm-iCOF(Br), EO-BIm-iCOF, and LITFSI@EO-BIm-iCOF (from left to right).

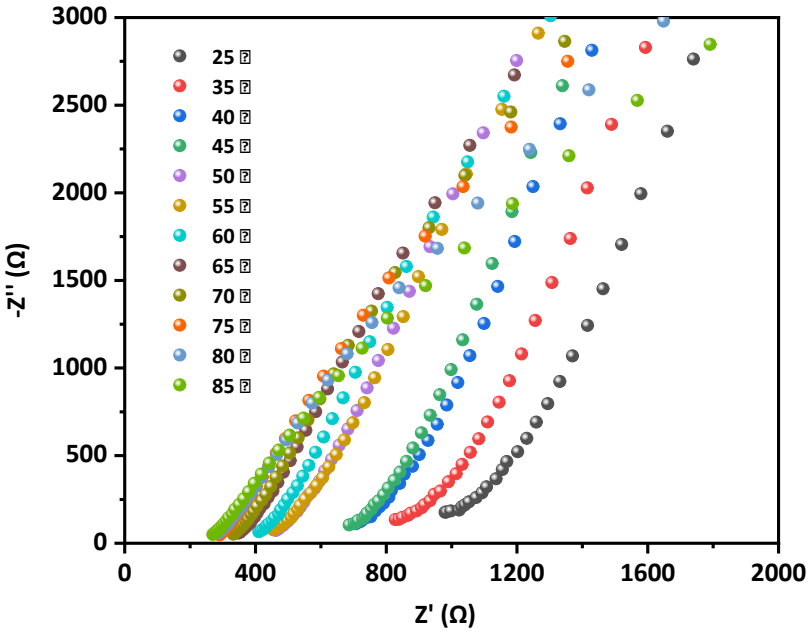

Fig. S16 The EIS spectra of LiTFSI@BIm-COF at various temperatures ranging from 25 ℃ to 85 ℃.

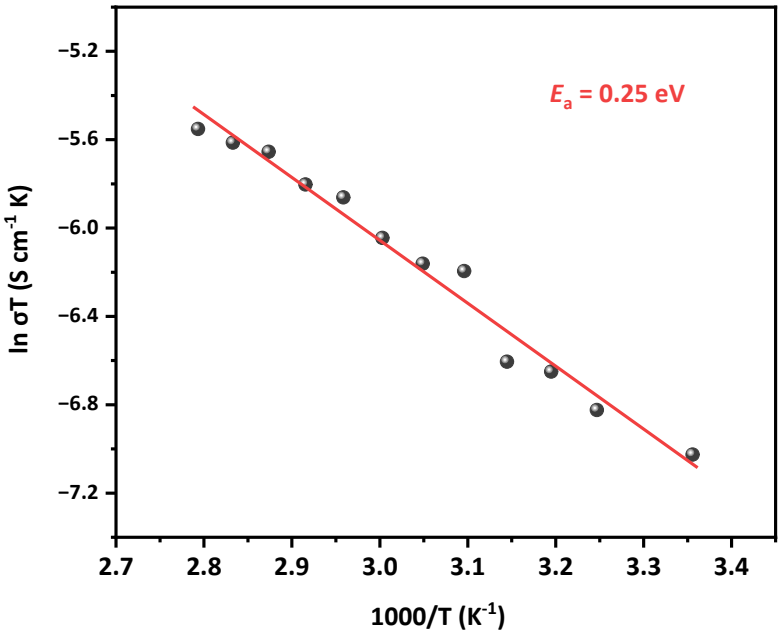

Fig. S17 Arrhenius plot of LiTFSI@BIm-COF at various temperatures ranging from 25 ℃ to 85 ℃.

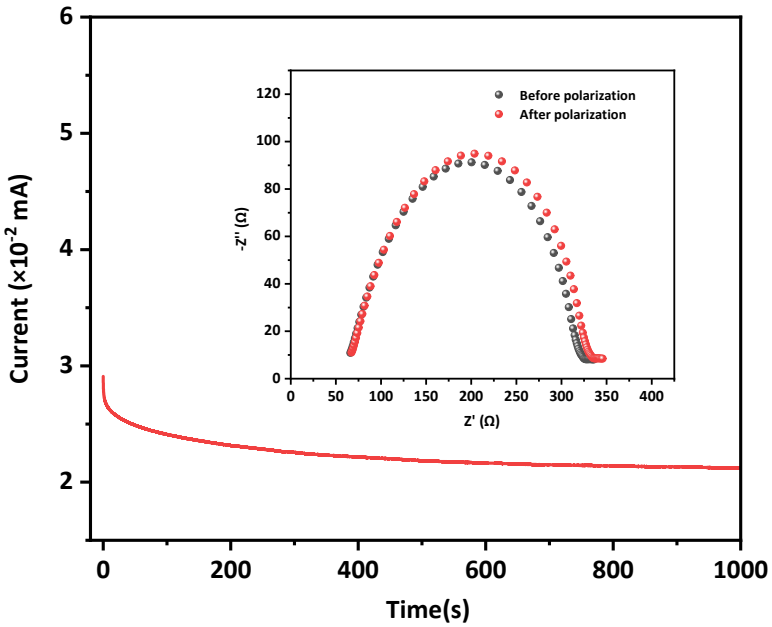

Fig. S18 Chronoamperometry curve of a Li||LiTFSI@BIm-COF||Li symmetric cell under 10 mV polarization at room temperature. Inset: EIS spectra before and after polarization, respectively.

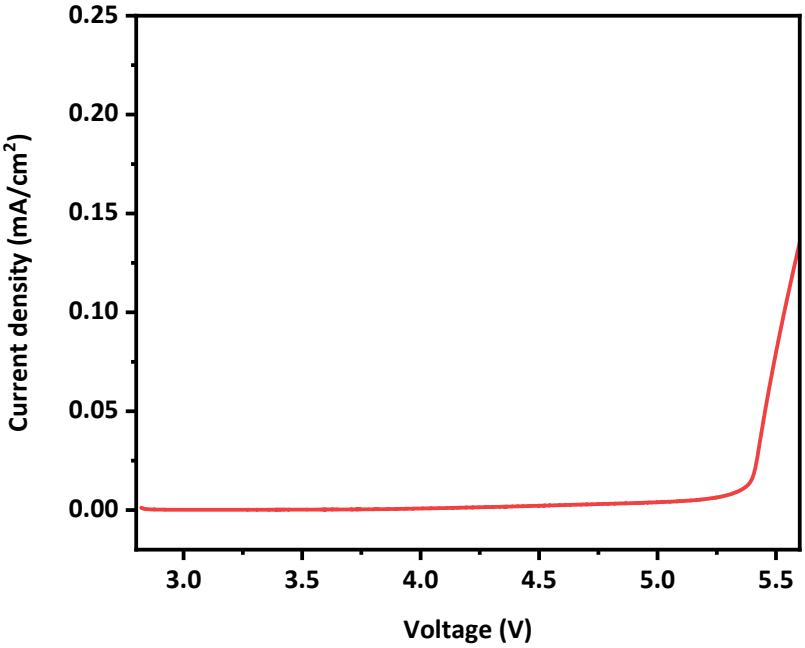

Fig. S19 LSV curve of the LiTFSI@BIm-COF at room temperature.

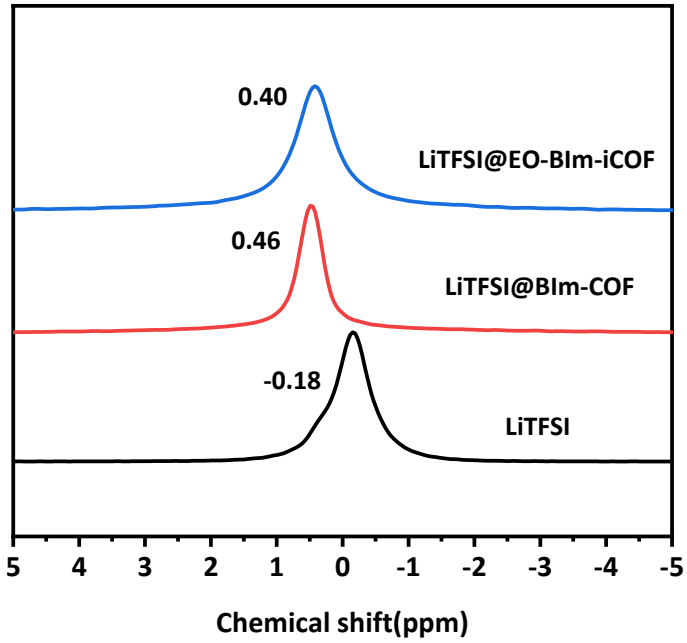

Fig. S20 ^{7}Li CP/MAS solid-state NMR spectra of pure LiTFSI salts, LiTFSI@BIm-COF, and LiTFSI@EO-BIm-iCOF.

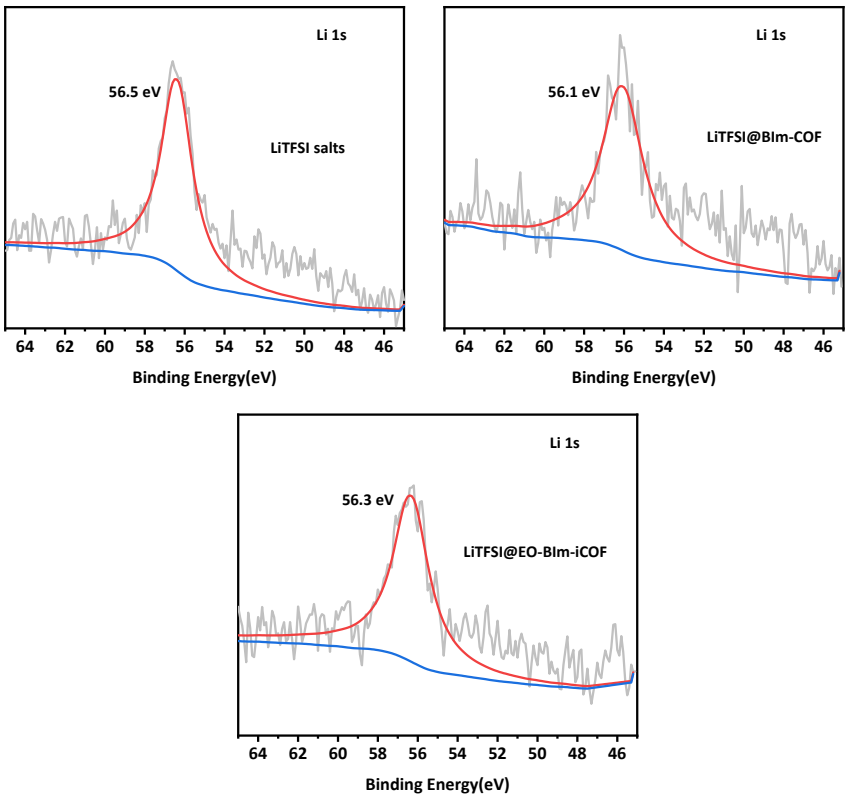

Fig. S21 Li 1s XPS spectra of pure LiTFSI salts, LiTFSI@BIm-COF, and LiTFSI@EO-BIm-iCOF.

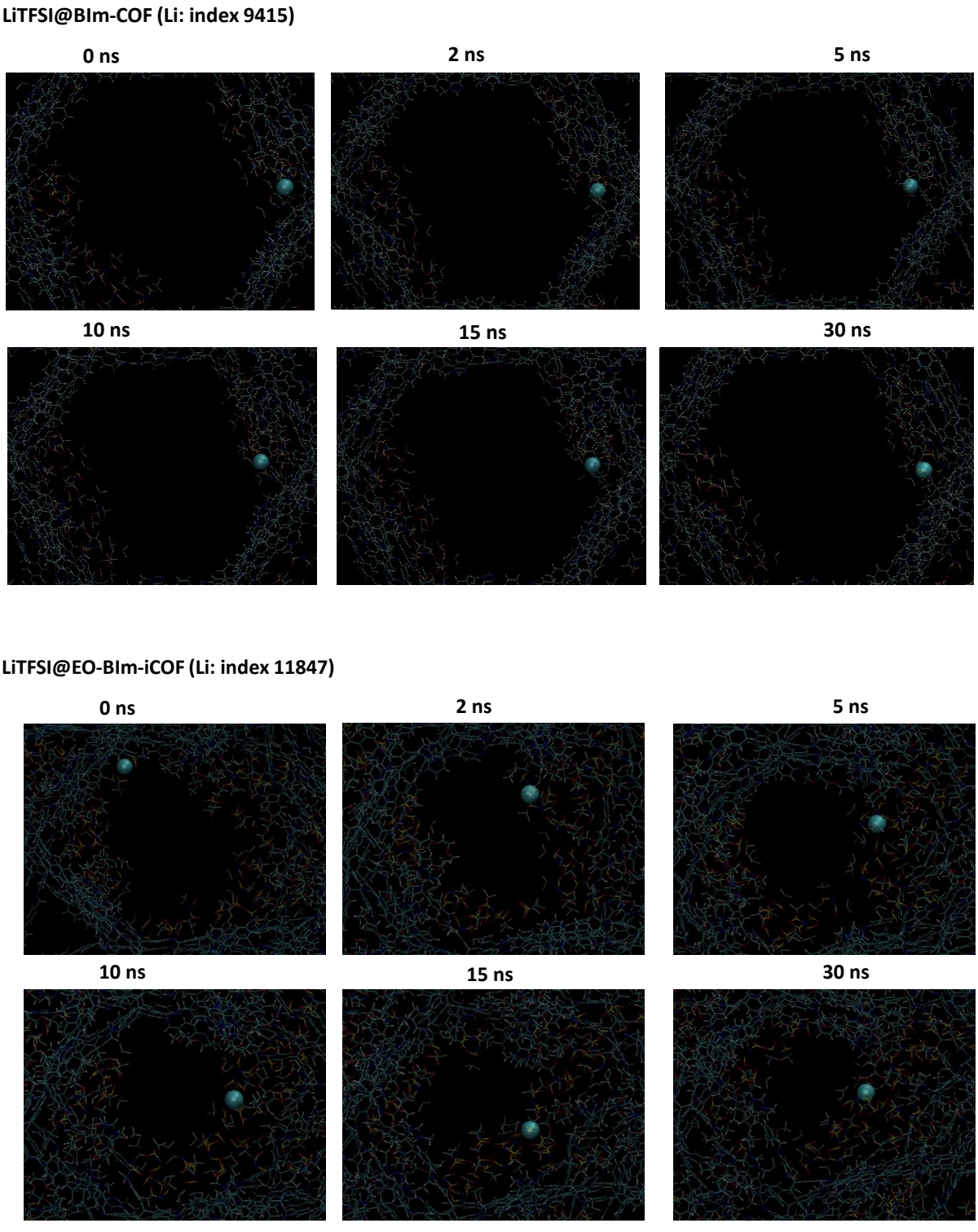

Fig. S22 Theoretical stimulation snapshots for the diffusion of Li^+ in LiTFSI@BIm-COF and LiTFSI@EO-BIm-iCOF, respectively.

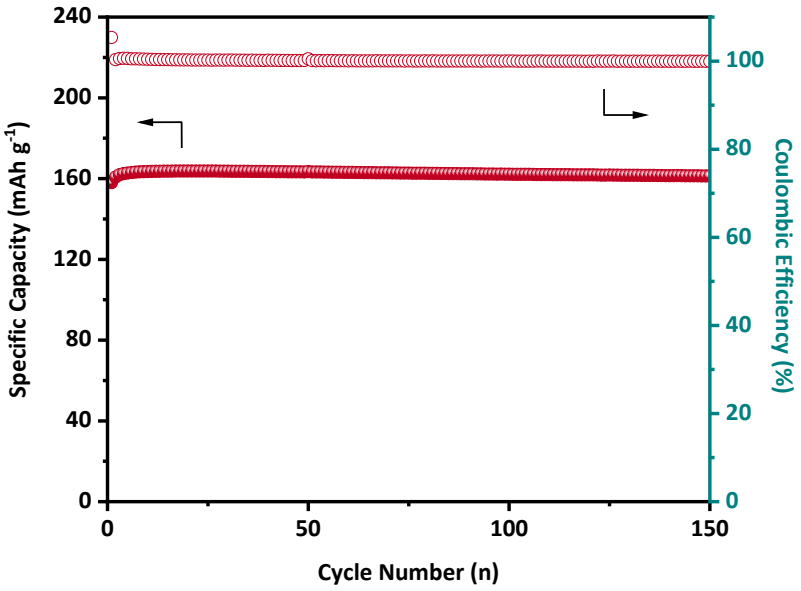

Fig. S23 Cycling stability and Coulombic efficiency of the $LiFePO_4$||LiTFSI@EO-BIm-iCOF||Li cell at a current density of 50 mA g^{-1} at 30 °C.

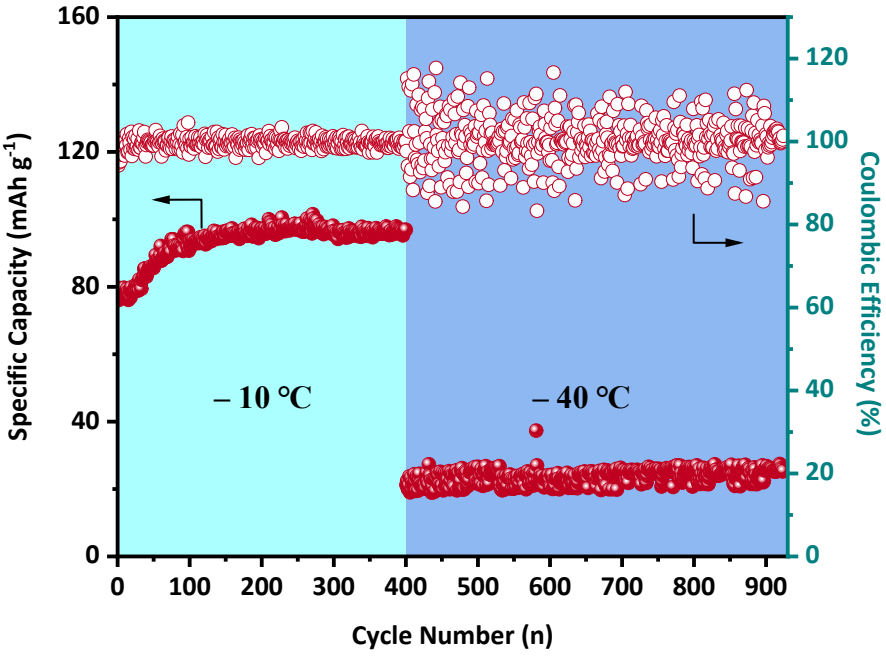

Fig. S24 Cycling stability and Coulombic efficiency of the LFP||LiTFSI@EO-BIm-iCOF||Li cell at 50 mA g^{-1} at -10 °C and -40 °C.

Table S1 The power density of LFP||LITFSI@EO-BIm-iCOF||Li and LFP||LITFSI@BIm-COF||Li battery

COFs SSEs	Current density ($A\ g^{-1}$)	Discharge capacities. ($mAh\ g^{-1}$)	Power density ($kW\ kg^{-1}$)
LITFSI@EO-BIm-iCOF	0.1	155.6	0.4
	0.2	150.4	0.7
	0.5	139.1	1.7
	1.0	126.1	3.3
	2.0	109.9	6.4
LITFSI@BIm-COF	0.1	135.4	0.3
	0.2	124.1	0.6
	0.5	96.6	1.5
	1.0	35.5	2.6
	2.0	0.1	3.8

References

[1] D. Van Der Spoel, E. Lindahl, B. Hess, G. Groenhof, A. E. Mark and H. J. C. Berendsen, *J. Comput. Chem.*, 2005, **26**, 1701.

[2] S. Páll, M. J. Abraham, C. Kutzner, B. Hess, E. Lindahl, in Lect. Notes Comput. Sci. (Including Subser. Lect. Notes Artif. Intell. Lect. Notes Bioinformatics), Springer, Cham, 2015, pp. 3-27.

[3] M. J. Abraham, T. Murtola, R. Schulz, S. Páll, J. C. Smith, B. Hess and E. Lindah, *SoftwareX*, 2015, **1-2**, 19.

[4] H. J. C. Berendsen, D. van der Spoel and R. van Drunen, *Comput. Phys. Commun.*, 1995, **91**, 43.

[5] W. L. Jorgensen, D. S. Maxwell and J. Tirado-Rives, *J. Am. Chem. Soc.*, 1996, **118**, 11225.

[6] Tian Lu and Feiwu Chen, *J. Comput. Chem.*, 2012, **33**, 580.